Light-Induced Phonon-Mediated Magnetization in Monolayer MoS_2

Shengjie Zhang(张圣杰)[1,2], Yufei Pei(裴昱非)[4], Shiqi Hu(胡史奇)[1], Na Wu(武娜)[1,2], Da-Qiang Chen(陈大强)[1,2], Chao Lian(廉超)[5,6], and Sheng Meng(孟胜)[1,2,3*]

[1]*Beijing National Laboratory for Condensed Matter Physics, and Institute of Physics, Chinese Academy of Sciences, Beijing 100190, China*
[2]*School of Physical Sciences, University of Chinese Academy of Sciences, Beijing 100190, China*
[3]*Songshan Lake Materials Laboratory, Dongguan 523808, China*
[4]*Department of Physics, University of Oxford, Oxford OX2 6QA, United Kingdom*
[5]*Oden Institute for Computational Engineering and Sciences, The University of Texas at Austin, Austin, Texas 78712, USA*
[6]*Department of Physics, The University of Texas at Austin, Austin, Texas 78712, USA*

(Received 13 April 2023; accepted manuscript online 29 May 2023)

Light-induced ultrafast spin dynamics in materials is of great importance for developments of spintronics and magnetic storage technology. Recent progresses include ultrafast demagnetization, magnetic switching, and magnetic phase transitions, while the ultrafast generation of magnetism is hardly achieved. Here, a strong light-induced magnetization (up to $0.86\mu_B$ per formula unit) is identified in non-magnetic monolayer molybdenum disulfide (MoS_2). With the state-of-the-art time-dependent density functional theory simulations, we demonstrate that the out-of-plane magnetization can be induced by circularly polarized laser, where chiral phonons play a vital role. The phonons strongly modulate spin-orbital interactions and promote electronic transitions between the two conduction band states, achieving an effective magnetic field ~ 380 T. Our study provides important insights into the ultrafast magnetization and spin-phonon coupling dynamics, facilitating effective light-controlled valleytronics and magnetism.

DOI: 10.1088/0256-307X/40/7/077502

Since the discovery of two-dimensional (2D) ferromagnetism in 2017,[1,2] searching and manipulating the magnetic properties in 2D materials have attracted a great deal of interests,[3–5] considering their immense potential in both fundamental physics such as the theory of low-dimensional magnetic orders and industrial applications. With the rapid development of laser pulse technology, photoexcitation has become an effective approach to control the properties of materials without disturbing the materials. Light control of magnetism in subpicosecond time scale has emerged as a highly active field since the first experimental observation[6] of ultrafast demagnetization in 1996. For comparison, it is worth noting that magnetization can also be manipulated using a static magnetic field with a timescale as short as 10 ps.[7] The ultrafast magnetic manipulation paves the way for the development of ultrafast spintronics and storage technology. Although lots of progresses have made on using ultrafast laser to achieve ultrafast demagnetization,[8–12] magnetization switching,[13–17] and magnetic phase transitions,[18–21] the generation of magnetism with ultrafast photoexcitation is still a challenge.

Here, we demonstrate an approach of generating magnetism using ultrafast laser pulses. Based on the real-time-dependent density functional theory (rt-TDDFT),[22] we investigate the light-induced magnetization in monolayer molybdenum disulfide (MoS_2), which has been adopted as a model 2D material with strong spin-orbit coupling (SOC), unique spin structure and good optical response.[23–26] The simulations reveal the emergence of a strong out-of-plane magnetization under circular polarized illumination. More interestingly, we find that the generation of magnetic moment is significantly enhanced (~ 10 times) by the presence of chiral phonons associated with the E'' phonon mode.[27] A two-level model analysis reveals that the chiral phonons act as an effective magnetic field ($\boldsymbol{B}_{\rm eff}$) originating from the SOC, which enhances spin flip between two conduction-band-minimum (CBM) states, resulting in a much strong magnetic moment in MoS_2. We estimate that the effective magnetic field induced by the chiral phonon can reach ~ 376 T, which is much stronger than the strongest steady magnetic field generated with a high-temperature superconducting magnet.[28] Finally, we demonstrate how to use the optical field to control the number of excited electrons and further the strength of magnetism.

The state-of-the-art real-time-dependent density functional theory simulations are performed using the home-built time-dependent *ab initio* package (TDAP) code.[29] The electron evolution is described by the time-dependent Kohn–Sham equation[30]

$$i\hbar\frac{\partial}{\partial t}|\psi_{n,\boldsymbol{k}}\rangle = \hat{H}|\psi_{n,\boldsymbol{k}}\rangle = \left[\frac{1}{2m}[\hat{\boldsymbol{p}} + e\boldsymbol{A}(t)]^2 + v + v_{\rm SOC}\right]|\psi_{n,\boldsymbol{k}}\rangle, \quad (1)$$

where $|\psi_{n,\boldsymbol{k}}\rangle$ is the two-component spinors. $\boldsymbol{A}$ is the vector

*Corresponding author. Email: smeng@iphy.ac.cn
© 2023 Chinese Physical Society and IOP Publishing Ltd

potential of the applied laser. We apply the dipole approximation and disregard the spatial dependence of the vector potential,[31] since the wavelength of the applied laser in this work is much greater than the size of a unit cell. The effective potential $v = v_{\rm H} + v_{\rm XC}$ includes the Hartree potential $v_{\rm H}$ and the exchange-correlation potential $v_{\rm XC}$. The last term $v_{\rm SOC} = \frac{e\hbar}{4m^2c^2}\hat{\boldsymbol{\sigma}} \cdot [\nabla v \times (\hat{\boldsymbol{p}} + e\boldsymbol{A})]$ is the potential for spin-orbit interaction, where c is the speed of light and $\hat{\boldsymbol{\sigma}}$ is the Pauli spin operator. The atomic nuclei move classically following Newton's law, whose forces can be calculated by Ehrenfest theorem:[32]

$$M_j \ddot{\boldsymbol{R}}_j = \sum_{n,\boldsymbol{k}} \langle |\psi_{n,\boldsymbol{k}}| \nabla_{\boldsymbol{R}_j} \hat{H} |\psi_{n,\boldsymbol{k}}\rangle, \tag{2}$$

where M_j and R_j denote the mass and position of the jth nucleus, respectively, and $\hat{H}$ is the Hamiltonian in Eq. (1). The dynamics of z-component of the magnetic moment reads

$$\frac{\partial}{\partial t} M_z(t) = -i\hbar\mu_{\rm B} \int \langle [\hat{H}, \sigma_z \hat{n}(\boldsymbol{r})] \rangle d\boldsymbol{r}, \tag{3}$$

where $\mu_{\rm B}$ is Bohr magneton, σ_z is the z-component of the Pauli spin operator, and $\hat{n}(\boldsymbol{r})$ is the density operator. In the first-principles calculations we utilized a k-point grid of $15 \times 15 \times 1$, a time step of 0.24 fs, and a relativistic projector-augmented-wave method. The total energy convergence criterion of 10^{-6} eV was adopted. To prevent artificial interlayer interactions for a 2D material, a vacuum layer of 20 Å was adopted in the calculations.

Light-Induced Magnetization in Monolayer MoS_2. In monolayer MoS_2, the valence and conduction bands have an energy splitting around 160 meV and 3 meV, respectively, due to the inversion asymmetry and strong SOC effects.[33–35] Similar to the Zeeman effect, the SOC acts as the effective magnetic field by controlling the direction of spin near the K/K' valley with respect to the out-of-plane direction (z direction).[23,26] Strong SOC and valley polarization provide the possibility of using circularly polarized light to control the spin degrees of freedom in monolayer MoS_2.

Figure 1(a) shows the band structure of monolayer MoS_2 and electron transition under a circularly polarized laser pulse around K and K' valleys. With a right-handed circularly polarized laser, the electrons in the K valley are excited from the valence band maximum (VBM) states to the CBM states. In contrast, the electrons in the $-K$ valley do not interact with the laser due to the chiral optical valley selection rule,[23,26] enabling the valley and spin selection upon photoexcitation. The corresponding magnetic moments along z direction, $M_z(t)$, are illustrated in Fig. 1(b) as a function of time. At a low laser intensity, there is no noticeable out-of-plane magnetic moment showing up in the photoexcited material. However, as the peak amplitude of laser electric field E_0 exceeds 0.015 V/Å, an increasingly pronounced $M_z(t)$ emerges in the initially non-magnetic system. When E_0 reaches 0.018 V/Å, we observe the laser-induced magnetic moment that attains a maximum value of 0.09 $\mu_{\rm B}$/f.u.

According to Eq. (3), the generation of magnetization is a direct result of the strong SOC in monolayer MoS_2, since the integral over the Poisson brackets in Eq. (3) is zero: $\int \langle [\hat{H}, \sigma_z \hat{n}(\boldsymbol{r})] \rangle d\boldsymbol{r} = 0$, that is, the $M_z(t)$ remains 0 when the SOC is absent. In Eq. (1), there is no direct coupling between light and spin, light can only scatter electrons into states with the same spin direction. When the laser is too weak to disturb the eigenstates of the states, excited electrons would stay in the higher CBM state, and would not transfer to the lower CBM state with opposite spins. The result is that magnetism cannot be generated. However, as the intensity of the laser increases, the CBM states of the ground state are no longer the eigenstates of the system even after the laser illumination. Thus, the excited electrons at the upper CBM state would steadily evolve into the lower CBM state. Since the spins of the electrons at the two CBM states are in opposite directions, the total spin of the system changes with time. Therefore, a net magnetic moment is observed during the relaxation process of photoexcited electrons.

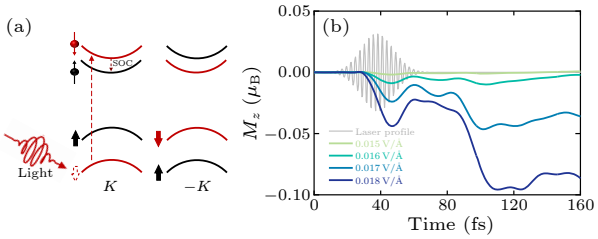

Fig. 1. Circularly polarized laser induces out-of-plane magnetization in monolayer MoS_2. (a) The ultrafast lasers with frequency matching that of the band gap of the material excites electrons in K valley from the VBMs to the CBMs. The splitting in the conduction band is exaggerated. The light of a particular polarization can only excite electrons in one valley. The communication between two CBMs is driven by the spin orbit coupling. (b) The gray line is the electric field of the applied laser pulse with full width at half maximum (FWHM) of 9.7 fs. The rest lines show the dynamics of the z-component of the total magnetic moment with varying laser intensity. The maximum magnetic momentum of 0.09$\mu_{\rm B}$ is induced with the applied laser of $E_0 = 0.018$ V/Å.

Chiral Phonon Enhanced Magnetization. We then introduce chiral phonons[36] to further control the spin dynamics in materials because the chiral phonons can further break the mirror symmetry.[37] Furthermore, the strong coupling between the chiral phonons associated with the E'' mode [Fig. 2(b)] and the spin, as well as its ability to break time-reversal symmetry,[38] enables us to select this chiral phonons for controlling the magnetism in MoS_2. Here, we consider the E'' mode chiral phonon for the strong coupling between this mode and spins.[27] We introduce the phonons in this system by displacing the initial positions of the sulfur atoms by an equal and opposite amount in the plane and giving them an in-plane initial velocity $\boldsymbol{v}$ perpendicular to the direction of displacement r with $|\boldsymbol{v}| = \omega r$, where $\hbar\omega = 43$ meV is the energy of the E'' phonon mode.[27] It should be noted that we artificially introduce the chiral phonons into our study. In experiment, the coherent phonons can be generated by electron–phonon coupling in the electronic excited state upon laser excitation, or by nonlinear phonons driven by strong mid-infrared or terahertz excitation.[18,39]

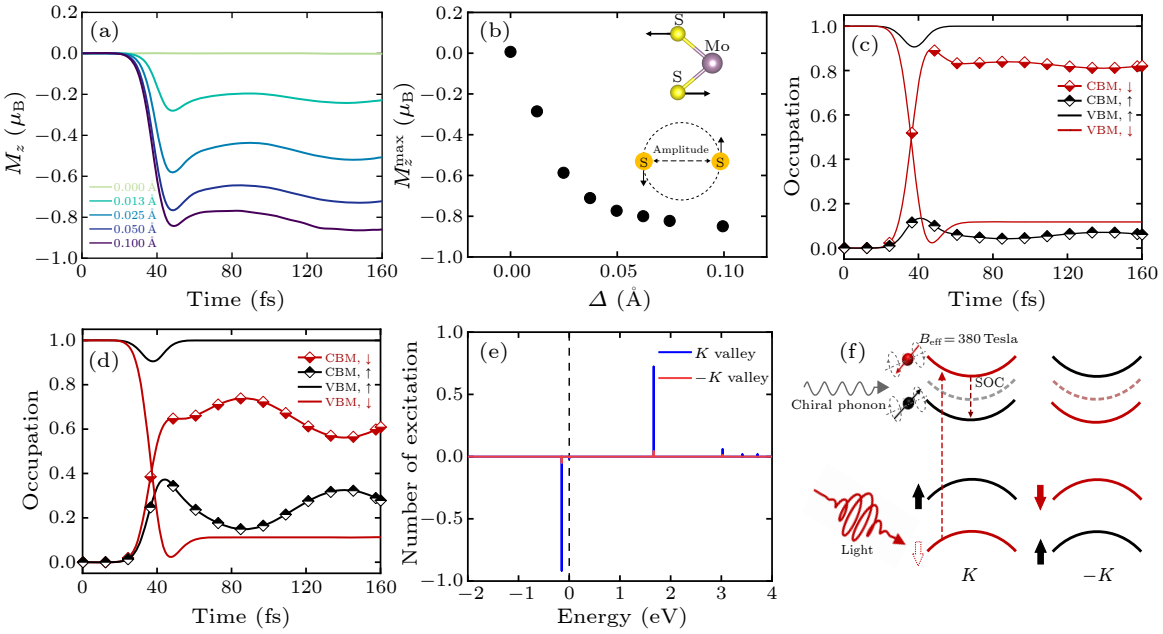

Fig. 2. The dynamics of magnetic moment is signally manipulated by chiral phonons. (a) Out-of-plane magnetization against phonon amplitude with light intensity fixed at $E_0 = 0.015\,\mathrm{V/Å}$. (b) The amplitude of phonons against out-of-plane magnetization with the same light intensity as in (a). The upper inset depicts the E'' phonon mode and the lower one is the motion of two sulfur atoms in a chiral phonon. [(c), (d)] Evolutions of occupation of CBMs and VBMs for $\Delta = 0.0\,\mathrm{Å}$ and $\Delta = 0.1\,\mathrm{Å}$, respectively. The arrows indicate the direction of spins, and the half-filled diamonds represent the occupations of CBMs. (e) The excitation in K and $-K$ valley when $t = 80\,\mathrm{fs}$. Lines with positive values represent an increase in the number of electrons, while lines with negative values represent a decrease in the number of electrons, forming electron holes. (f) A schematic diagram illustrating the phonon influence on spin dynamics. The presence of phonons causes two CBM states no longer to be eigenstates, thus enhancing electron transitions between the two states.

Figure 2(a) shows the evolution of out-of-plane magnetization when E_0 is fixed at $0.015\,\mathrm{V/Å}$. Interestingly, the chiral phonons can dramatically enhance the light-induced magnetization, even if the laser field is too weak ($E_0 = 0.015\,\mathrm{V/Å}$) to generate net magnetization in the system when the atoms are fixed. We can observe obvious magnetic moment [Fig. 2(a)] when chiral phonons exist, indicating a significant contribution of the laser-induced magnetic moment by the chiral phonons. Moreover, with the increasing phonon amplitudes Δ, the magnetism generation under a weak laser field can be greatly enhanced.

More details are shown in Fig. 2(b), where the maximum magnetization within the first phononic period is plotted against the amplitude of the chiral phonon. As the phonon mode is gradually turned on, the magnitude of the magnetization increases and saturates at $\sim 0.85\mu_B$/f.u. when Δ reaches 0.1 Å. Noticeably, without chiral phonons, the maximum magnetic moment we obtained is only $0.09\mu_B$ as discussed above, when the optical intensity was set to $0.018\,\mathrm{V/Å}$.

To investigate the mechanism of the phonon enhanced magnetization, we track the occupations of excited electrons/holes as a function of time during the photoexcitation with and without the E'' phonon in Figs. 2(c) and 2(d). The occupation is defined as

$$\mathrm{occ}_{n,\boldsymbol{k}} = \sum_{n'} |\langle \phi_{n,\boldsymbol{k}} | \psi_{n',\boldsymbol{k}} \rangle|^2,$$

where $|\phi_{n,\boldsymbol{k}}\rangle$ is the initial eigenstate of the system.

The energy of the chiral phonon is only 43 meV, which is insufficient to excite electrons from the valence band to the conduction band (band gap = 1.54 eV). Therefore, the phonon has almost no impact on the electron transitions between the conduction and valence bands. As shown in Figs. 2(c) and 2(d), the occupations of down-spin valence bands are almost the same.

Without chiral phonons, there are only electronic transitions between states with the same spin, consistent with what we mentioned above. Therefore, the total magnetic moment of the system remains unchanged. However, the energy of phonon mode is comparable to the difference of the energy between the two CBM states, which implies that phonons can couple non-adiabatically with two CBM states and open the channel for electrons to transition between two CBM states. In Fig. 2(d), we demonstrate the electron transitions from the upper CBM states to the lower ones. Similar processes have been discussed in Ref. [40]. Since the energy of phonon mode corresponds to 43 meV, the energy difference between two VBM states is about 160 meV, and the energy of phonons is not high enough to make electronic transition between the two VBMs. Therefore, there is no spin flip for holes after photoexcitation. Moreover, we simultaneously include both K and $-K$ valleys in our calculation. Using circularly polarized light, we see clearly that only $+K$ valley is excited and no photoexcitation at the $-K$ valley. On the

other hand, Fig. 2(e) shows that there is no inter-valley scattering because the coherent phonon is at the Γ point only and thermal phonons can be ignored at low temperatures. Consequently, the electrons in one valley occupy more spin-down states and fewer spin-up states, resulting in generation of magnetization.

Furthermore, this chiral-phonon-enhanced magnetization can be understood from the viewpoint of the spin dynamics in an effective magnetic field. We introduce a phenomenological Hamiltonian to describe the evolution of spin states in CBMs:

$$\hat{H}_{\rm B} = \frac{e\hbar}{2m}\hat{\boldsymbol{\sigma}}\cdot\boldsymbol{B}_{\rm eff}(t), \tag{4}$$

where $\boldsymbol{B}_{\rm eff}(t) = \frac{1}{2mc^2}\nabla_{\boldsymbol{r}} v(\boldsymbol{R},\rho(t)) \times (\hat{\boldsymbol{p}} + e\boldsymbol{A})$ is the effective magnetic field that arises from SOC and $\rho(t)$ is the time-dependent electric charge density. The energy splitting of 3 meV between two CBM states results from the effective magnetic field in the ground state. The chiral phonons could adjust the SOC by modulating the potential term $v(\boldsymbol{R},\rho)$ and the moment of electrons. In the ground state of monolayer MoS_2, the effective magnetic field is perpendicular to the 2D material due to the spin directions of the CBM states pointing along the z-direction. Since spins stay in the eigenstates, when they are parallel or antiparallel to the magnetic field, such a field cannot change the direction of the spins. By contrast, the chiral phonons can provide an additional field,[38,41,42] which opens a channel for electronic transitions between two CBM states. As shown in Fig. 2(d), the occupation in CBMs evolves periodically with a period of $T = 95$ fs. According to the two-level model of spins in a magnetic field, the frequency of the occupation oscillation is $\omega = \frac{2\pi}{T} = \frac{2\mu_{\rm B}|\boldsymbol{B}_{\rm eff}|}{\hbar}$.[43] We determine the strength of the effective field to be $|\boldsymbol{B}_{\rm eff}| \approx 376$ T, which is approximately fifteen times stronger than the magnetic field $|\boldsymbol{B}_{\rm g}| \approx 26$ T induced by SOC at CBMs in the ground state. The effective field $|\boldsymbol{B}_{\rm eff}| \approx 376$ T also agrees with the energy splitting of ~ 40 meV between two CBM states observed in the laser excited state.

Recently, there have been productive discussions about ultrafast magnetization.[44,45] What distinguishes our work from these works is that our work points out that the generation of magnetism is due to the transition of electrons between two CBM states. Furthermore, we point out that chiral phonons play a role in generating an effective magnetic field of 376 T during magnetism generation, and their existence significantly enhances the magnetic moment.

Modulation of Magnetization with Light. To study the method of using light fields to control the final magnetic moment, we investigate the magnetic moment in monolayer MoS_2 under different light field intensities. In Fig. 3(a), we show the laser intensity dependence of magnetic moment at a fixed amplitude of phonons with the position displacement of 0.013 Å. Upon laser excitation, a transient non-zero magnetic moment is induced within 50 fs. Unlike the inverse Faraday effect,[46] the final magnetic moments do not simply increase with the enhancement of the light field. When the intensity of the laser exceeds 0.022 V/Å, the magnetic moment begins to decrease after reaching its maximum, leading to the residual magnetization substantially smaller than the weak field case. However, with $E_0 = 0.036$ V/Å, the magnetization first decreases and reaches a minimum at 46 fs, then increases again, and ultimately reaches a final magnetization strength similar to that achieved with $E_0 = 0.015$ V/Å.

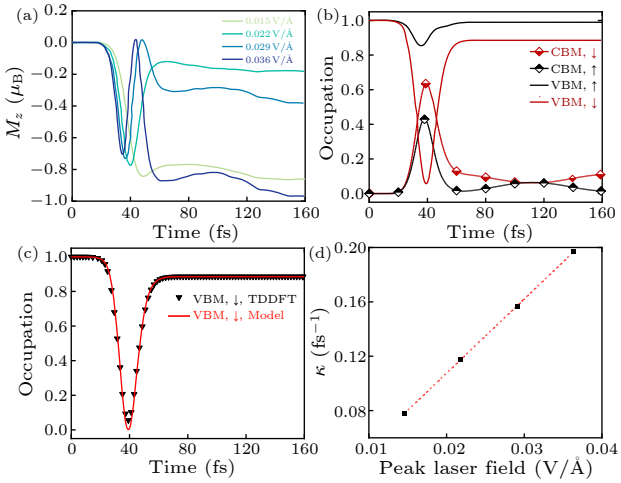

Fig. 3. Modulation of magnetization with light. (a) The time-dependent evolution of magnetization under light of different intensities. (b) The occupation with light intensity of $E_0 = 0.022$ V/Å and chiral phonons. The amplitude of the chiral phonons is $\Delta = 0.1$ Å in (a) and (b). (c) The occupations of upper VBM state obtained by using TDDFT (black triangles) and the two-band model (red line). (d) Peak laser field vs transitional amplitude κ in Eq. (8).

We attribute the behavior of magnetic moment varying with light field intensity to the electronic transitions between the CBM state and VBM states. Figure 3(b) displays the corresponding dynamics of the electron occupation with $E_0 = 0.022$ V/Å. We observe the occupation of VBM states evolving in a similar way to the magnetization. Finally, almost no electrons remain in the CBM states.

These behaviors can be explained by a simple two-level model. We write the wavefunction as $|\psi\rangle = c_1|\phi_1\rangle + c_2|\phi_2\rangle$, where $|\phi_1\rangle$ and $|\phi_2\rangle$ are the VBM and CBM eigenstates in the interaction picture respectively, and $|c_1|^2 + |c_2|^2 = 1$. Then we obtain

$$i\hbar\dot{c}_i = V_{ii}c_i + V_{ij}e^{i\omega_{ij}t}c_j, \tag{5}$$

where $i, j = 1, 2$ and $i \neq j$. V_{ij} are transition matrix elements, and $\omega_{21} = -\omega_{12} = \Delta E/\hbar$ is the frequency corresponding to the band gap ΔE at the K valley. We add perturbation that behaves the same as the laser field in Fig. 1(b). The perturbation Hamiltonian reads

$$\Delta\hat{H} = \begin{bmatrix} 0 & V_{12} \\ V_{21} & 0 \end{bmatrix}, \tag{6}$$

where $V_{12} = V_{21}^* = \kappa\hbar\exp[-\frac{(t-t_0)^2}{2\tau^2}]e^{i\omega t}$, and κ is a parameter measuring the intensity of the transition matrix, with t_0 and τ being the parameters that control the FWHM and the time when the maximum light intensity appears. If

the frequency of the light matches the band gap, $\omega = \omega_{21}$, Eq. (5) will then become

$$i\dot{c}_i = \kappa \exp\Big[-\frac{(t-t_0)^2}{2\tau^2}\Big]c_j. \tag{7}$$

The occupation of the upper VBM state can be integrated to be

$$|c_1|^2 = \cos^2\Big[\sqrt{\frac{\pi}{2}}\kappa\tau\,\mathrm{erf}\Big(\frac{t-t_0}{\sqrt{2}\tau}\Big) + \sqrt{\frac{\pi}{2}}\kappa\tau\,\mathrm{erf}\Big(\frac{t_0}{\sqrt{2}\tau}\Big)\Big], \tag{8}$$

where erf is the error function, and the phase is added to guarantee $|c_1(0)|^2 = 1$. If, on the other hand, the frequencies do not match, then the integrand will contain a rapidly oscillating phasor term that cancels out the integration and prevent the final occupation of the upper band. This is in accordance with expectation, as the transition of the lower VBM band is observed to be slow and eventually return to full occupation.

Table 1. Parameters κ, τ, and t_0, appearing in Eq. (8), for different laser intensities.

E_0 (V/Å)	κ (fs^{-1})	τ (fs)	t_0 (fs)
0.015	0.0776	9.707	38.44
0.022	0.1180	9.373	37.89
0.029	0.1566	9.536	37.87
0.036	0.1969	9.202	37.61

In Fig. 3(c), the occupation numbers obtained by using TDDFT and our two-band model with $E_0 = 0.022$ V/Å are in perfect agreement. Moreover, Fig. 3(d) displays the plot of E_0 vs κ in Eq. (6). One can see a clear linear relationship, which confirms that the transition amplitude is proportional to the external electric field.

While Eq. (8) reveals an oscillation in the occupation of VBMs with time, only one or two peaks can be observed since the laser pulse width is limited, as shown in Fig. 3(a). As shown by Eq. (8) and Table 1, the time for the first maximum becomes shorter with increasing light intensity, as the frequency is proportional to κ and E_0. Therefore, appropriate intensity and FWHM values are required to ensure that the occupation in the CBMs does not become zero when the laser pulse dissipates. Furthermore, different laser parameters can result in different occupations in CBMs, which allow us to tune the laser features to control the final occupation and, ultimately, the final magnetization. It is interesting to compare our results with the conventional[46,47] and ultrafast[44,48] inverse Faraday effect (IFE). Like IFE, when only laser light is introduced and the laser intensity is weak in our work, circularly polarized light can generate a magnetic moment in non-magnetic materials. Moreover, the magnitude of the net magnetic moment increases with the increase in light intensity. However, when chiral phonons are introduced into the system, it exhibits different characteristics from the conventional IFE. With increasing phonon amplitude, the magnetic moment significantly increases [Fig. 2(b)]. Our study reveals a unique method of creating magnetism in non-magnetic substances, which differs from the IFE that offers various means of manipulation.

It is worth noting that the above analysis is not limited to MoS_2 monolayers. Thin films of MoS_2 and other two-dimensional dichalcogenide materials would also experience the similar effects and dynamic behaviors under photoexcitation by intense circularly polarized lasers. Moreover, materials with heavier elements, such as WSe_2, have a much stronger SOC[49–51] and would, therefore, produce even stronger effective magnetic fields.

In conclusion, our study has demonstrated a laser-induced magnetization up to $0.85\mu_B$/f.u. in non-magnetic MoS_2 layers. By exciting electrons in the K valley from VBMs to CBMs with strong ultrafast laser pulses, we can obtain a nonzero magnetization. The chiral phonons associated with E'' phonon mode promote the communication between two CBMs with different spins, resulting in a much stronger magnetization. Furthermore, the magnitude of the maximum achievable magnetization is positively correlated with phonon amplitude, but it is not simply correlated with light field intensity. A potential way of controlling such a magnetization is proposed, i.e., by using consecutive lights with identical or different polarizations to excite the material. Our results suggest a promising approach for generating 2D magnetism in dichalcogenide 2D materials, with potential applications in valleytronics and engineering, and may also serve as a foundation for further studies on the interplay between phonons and spins.

We thank Professor Baoli Liu for helpful discussion. This work was supported by the National Key R&D Program of China (Grant No. 2021YFA1400201), the National Natural Science Foundation of China (Grant Nos. 12025407 and 11934004), and Chinese Academy of Sciences (Grant Nos. XDB330301 and YSBR047).

References

[1] Huang B, Clark G, Navarro-Moratalla E *et al.* 2017 *Nature* **546** 270
[2] Gong C, Li L, Li Z *et al.* 2017 *Nature* **546** 265
[3] He J J and Frauenheim T 2020 *J. Phys. Chem. Lett.* **11** 6219
[4] Deng Y J, Yu Y J, Song Y C *et al.* 2018 *Nature* **563** 94
[5] O'Hara D J, Zhu T, Trout A H *et al.* 2018 *Nano Lett.* **18** 3125
[6] Beaurepaire E, Merle J C, Daunois A, and Bigot J Y 1996 *Phys. Rev. Lett.* **76** 4250
[7] Kirilyuk A, Kimel A V, and Rasing T 2010 *Rev. Mod. Phys.* **82** 2731
[8] Krieger K, Elliott P, Muller T, Singh N, Dewhurst J K, Gross E K U, and Sharma S 2017 *J. Phys.: Condens. Matter* **29** 224001
[9] Chekhov A L, Behovits Y, Heitz J J F *et al.* 2021 *Phys. Rev. X* **11** 041055
[10] Tauchert S R, Volkov M, Ehberger D *et al.* 2022 *Nature* **602** 73
[11] Mishra K, Rowan-Robinson R M, Ciuciulkaite A, Davies C S, Dmitriev A, Kapaklis V, Kimel A V, and Kirilyuk A 2022 *Nano Lett.* **22** 9773
[12] Zhang W, Lin J X, Huang T X, Malinowski G, Hehn M, Y X, Mangin S, and Zhao W 2022 *Phys. Rev. B* **105** 054410
[13] Zhang P Y, Chung T F, Li Q W *et al.* 2022 *Nat. Mater.* **21** 1373
[14] Jakobs F and Atxitia U 2022 *Phys. Rev. Lett.* **129** 037203
[15] Stupakiewicz A, Davies C S, Szerenos K, Afanasiev D, Rabinovich K S, Boris A V, Caviglia A, Kimel A V, and Kirilyuk A 2021 *Nat. Phys.* **17** 489

[16] Selzer S, Salemi L, Deák A, Simon E, Szunyogh L, Oppeneer P M, and Nowak U 2022 *Phys. Rev. B* **105** 174416
[17] Lefkidis G and Hübner W 2007 *Phys. Rev. B* **76** 014418
[18] Disa A S, Fechner M, Nova T F, Liu B, Först M, Prabhakaran D, Radaelli P G, and Cavalleri A 2020 *Nat. Phys.* **16** 937
[19] Nova T F, Cartella A, Cantaluppi A, Först M, Bossini D, Mikhaylovskiy R V, Kimel A V, Merlin R, and Cavalleri A 2016 *Nat. Phys.* **13** 132
[20] You W J, Tengdin P, Chen C *et al.* 2018 *Phys. Rev. Lett.* **121** 077204
[21] Li G, Medapalli R, Mentink J H *et al.* 2022 *Nat. Commun.* **13** 2998
[22] Runge E and Gross E K U 1984 *Phys. Rev. Lett.* **52** 997
[23] Xiao D, Liu G B, Feng W, X X, and Yao W 2012 *Phys. Rev. Lett.* **108** 196802
[24] Zhu C R, Zhang K, Glazov M, Urbaszek B, Amand T, Ji Z W, Liu B L, and Marie X 2014 *Phys. Rev. B* **90** 161302(R)
[25] Kumar A, Yagodkin D, Stetzuhn N, Kovalchuk S, Melnikov A, Elliott P, Sharma S, Gahl C, and Bolotin K I 2021 *Nano Lett.* **21** 7123
[26] Cao T, Wang G, Han W *et al.* 2012 *Nat. Commun.* **3** 887
[27] Cai Y Q, Lan J H, Zhang G, and Zhang Y W 2014 *Phys. Rev. B* **89** 035438
[28] Hahn S, Kim K, Kim K *et al.* 2019 *Nature* **570** 496
[29] Lian C, Guan M, S H, Zhang J, and Meng S 2018 *Adv. Theory Simul.* **1** 201800055
[30] Ullrich C A 2011 *Time-Dependent Density-Functional Theory Concepts and Applications* (Oxford: Oxford University Press)
[31] Krieger K, Dewhurst J K, Elliott P, Sharma S, and Gross E K U 2015 *J. Chem. Theory Comput.* **11** 4870
[32] Bornemann F A, Nettesheim P, and Schutte C 1996 *J. Chem. Phys.* **105** 1074
[33] Zhu Z Y, Cheng Y C, and Schwingenschlögl U 2011 *Phys. Rev. B* **84** 153402
[34] Shi H L, Pan H, Zhang Y W, and Yakobson B I 2013 *Phys. Rev. B* **87** 155304
[35] Kadantsev E S and Hawrylak P 2012 *Solid State Commun.* **152** 909
[36] Zhang L F and Niu Q 2015 *Phys. Rev. Lett.* **115** 115502
[37] Du L J, Tang J, Zhao Y C *et al.* 2019 *Adv. Funct. Mater.* **29** 1904734
[38] Shin D, Hubener H, De Giovannini U, Jin H, Rubio A, and Park N 2018 *Nat. Commun.* **9** 638
[39] Disa A S, Nova T F, and Cavalleri A 2021 *Nat. Phys.* **17** 1087
[40] Jiang X, Zheng Q J, Lan Z G, Saidi W A, Ren X G, and Zhao J 2021 *Sci. Adv.* **7** eabf3759
[41] Juraschek D M, Narang P, and Spaldin N A 2020 *Phys. Rev. Res.* **2** 043035
[42] Juraschek D M, Neuman T, and Narang P 2022 *Phys. Rev. Res.* **4** 013129
[43] Griffiths D J and Schroeter D F 2018 *Introduction to Quantum Mechanics* (New York: Prentice Hall)
[44] Okyay M S, Kulahlioglu A H, Kochan D, and Park N 2020 *Phys. Rev. B* **102** 104304
[45] Neufeld O, Tancogne-Dejean N, De Giovannini U, Hübener H, and Rubio A 2023 *npj Comput. Mater.* **9** 39
[46] Hertel R 2006 *J. Magn. Magn. Mater.* **303** L1
[47] Pershan P S, van der Ziel J P, and Malmstrom L D 1966 *Phys. Rev.* **143** 574
[48] Mikhaylovskiy R V, Hendry E, and Kruglyak V V 2012 *Phys. Rev. B* **86** 100405
[49] Yun W S, Han S W, Hong S C, Kim I G, and Lee J D 2012 *Phys. Rev. B* **85** 033305
[50] Yeh P C, Jin W, Zaki N *et al.* 2015 *Phys. Rev. B* **91** 041407
[51] Kumar A and Ahluwalia P K 2012 *Eur. Phys. J. B* **85** 186